Estimation of S-wave velocity structure of deep soils using waveform inversion for S-wave part of earthquake ground motion from small event.

Haruhiko Suzuki[1] and Hiroaki Yamanaka[2]

[1] *Oyo Corporation, Japan*
[2] *Tokyo Institute of Technology, Japan*
Email: suzuki-haruhiko@oyonet.oyo.co.jp, yamanaka@depe.titech.ac.jp

ABSTRACT :

We propose an inversion method for estimation of a 1D S-wave velocity structure of deep sedimentary layers using S-wave parts of earthquake records for evaluating site amplification. Genetic algorithm is used in inversion to find an optional model that has the minimum misfit between observed and calculated S-waves. We conducted numerical experiments using synthetic data. We applied our method to actual data at Narita in the Kanto basin and at stations around Lake Biwa. Effectiveness of the proposed methods were confirmed in the numerical experiments and actual applications

KEYWORDS: S-wave, S-wave velocity structure, genetic algorithm, waveform inversion

1. INTORDUCTION

It is important to evaluate characteristics of source, path and site effects for strong motion prediction. S-wave velocity structure is one of the most important factors. Recently many 3D subsurface structural models were constructed for strong motion estimation (e.g., Horikawa et al., 2003; Yamanaka and Yamada, 2006). These models were constructed using reflection, refraction and microtremor array surveys. Although there are many geophysical data in urban area, there are a few data in small plains.

On the other hands, strong motion seismograph networks (K-NET) have been constructed in Japan after Hyogo-ken Nanbu earthquake in 1995 to cover whole of Japan. If an S-wave velocity structure can be constructed using these strong motion data, we can construct a 3D subsurface structural model in the area there are a few geophysical data.

Several methods are now available to construct the S-wave velocity structure using earthquake records, such as receiver function method (Kurose and Yamanaka,2006), phase velocity analysis of surface waves (Mikoshiba and Kinoshita,1989; Miura and Midorikawa,2001), group velocity analysis of surface waves (Yamanaka et al,1989) and spectral analysis between horizontal and vertical components of surface waves (Kudo and Sakaue,1984). Although it is important to estimate characteristics of S-wave for the strong motion prediction, the method to evaluate S-wave velocity structural model using S-wave parts of earthquake data. Hikima and Kokestu (2005) recently evaluated an S-wave velocity structural model using reflectivity method. Because non linear least square method is used in inversion process, it takes much amount of calculation at high frequency range. Furthermore we have to decide many parameters of source in their procedure.

In this study, we use smoothed ramp function for source time function in modeling S-wave part. In inversion process we use a genetic algorithm. Because of using simple source time function, we use small earthquake. At first, we perform the numerical experiment to applicability of the method. Then we applied our method to actual earthquake data at Narita in the Kanto basin and around Lake Biwa.

2. INVERSION METHOD

Concept of estimation of S-wave velocity structure in our method is displayed in Figure 2.1. We calculate velocity wave form at surface using Haskell method(Haskell,1960). Q-value is modeled in the form Eqn2.1.

$$Q_s = \frac{Vs}{a} f^b \qquad (2.1)$$

Here, Vs, f, a and b are S-wave velocity (m/s), frequency(Hz), constant, respectively.
Before inversion, we decide first brake of *t1*, *t2* and *t3* in Figure 2.1. Misfit *ei* between observed and calculated

waves of S-wave from *t1* to *t3* is defined in the form Eqn2.2. *τi* is defined to minimize *ei*.

$$e_i = \sum_{t=t1}^{t2}\left(\frac{O_i(t)}{A_i^o} - \frac{C_i(t+\tau_i)}{A_i^s}\right)^2 \tag{2.2}$$

Here, Oi, A_i^o, Ci, A_i^s are observed velocity wave, maximum amplitude of observed wave, calculated velocity wave, maximum amplitude of calculated wave, respectively. The misfit between observed and calculated waves from *t2* to *t3* is defined in the form Eqn2.3.

$$E = \sum_{i=1}^{M}\sum_{t=t2}^{t3}\left(\frac{O_i(t)}{A_i^o} - \frac{C_i(t+\tau_i)}{A_i^s}\right)^2 \tag{2.3}$$

Here, *M* is number of earthquake data. S-wave velocity structure is optimized to minimize *E*. Minimization of *E* is performed by genetic algorithm (GA). The parameters in the inversion are S-wave velocity and thickness of each layer, *a*, *b*, input angle and *Tr*. S-wave velocity of the basement is fixed. Density of each layer is calculated from *Vs* in the Eqn2.4(Ludwig et al.,1973).

$$\rho(g/cm^3) = -0.0450Vs^2 + 0.4316Vs + 1.7106(Vs \le 3.2)$$
$$\rho(g/cm^3) = 0.0448Vs^2 + 0.2481Vs + 1.3760(Vs > 3.2) \tag{2.4}$$

3. NUMERICAL EXPERIMENTS

3.1. S-wave velocity model and pseudo observed data
In numerical experiments, we use deep model (Model 1) and shallow model (Model 2, Model 3). These models are displayed in Figure 3.1. A band pass filter from 1sec to 5sec is used for synthetic observed data. The random phase noise with amplitude of 30% of its fourier specta is added. Input angles are 0degree (Event1-1), 30degree (Event1-2) and 45degree (Event1-3). *Tr* are 1.0s (Event1-1), 1.25s (Event1-2) and 1.5s (Event1-3) in the case of Model 1. Input angles are 0degree (Event2-1 and Event3-1), 10degree (Event2-2 and Event3-2) and 20degree (Event2-3 and Event3-3). *Tr* are 1.0s (Event2-1 and Event3-1), 1.25s (Event2-2 and Event3-2), 1.5s (Event2-3 and Event3-3) in the cases of Model 2 and Model 3.

3.2.Results
The four-layers model in used in the numerical experiments. Populations, generations, rate of crossover and rate of mutation are 200, 100, 0.7 and 0.01, respectively. Search area is displayed in Table 3.1.
Comparisons between observed and calculated waveforms are displayed in Figure 3.2a. Comparisons of parameters between true and inverted models are displayed in Figure3.2b. Calculated wave agree well observed wave. Parameter distributions of the acceptable models for the inversions in numerical experiment for Model1 are displayed in Figure 3.3. The threshold was set to be equal to the minimum *E**1.07. Rectangle areas indicate search areas of each parameter. S-wave velocities and thicknesses of the first, second and third layers are displayed in Figure 3.3a. These parameters agree well with the true model. *Tr* and input angle of Event1-1, Event1-2 and Event1-3 are displayed Figure 3.3b. a and b for Q-value are displayed in Figure 3.3c. Although *Tr* and input angle agree with true model, *a* and *b* for Q-value don't agree. Because of the band-pass filtering, Q-value could not be well estimated.
The results of the inversion with optimization of *t1* and *t3* for Model 1 are displayed in Figure 3.4. Calculated wave agree well with observed wave. The parameter distributions of acceptable models for the inversions in numerical experiment with optimization of *t1* and *t3* for Model1 are displayed in Figure 3.4. The threshold was set to be equal to the minimum *E**1.07. The S-wave velocity and thickness of each layer are more disarranged than that of Figure 3.2a. The sensitivity of the first S-wave is low for change of S-wave velocity structure. As the result of this numerical experiment, start time of calculating *E* is *t2*.

4. APPLICATON TO DATA AT NARITA IN KANTO BASIN
We applied our method to actual data at Narita(CHBH13) in the Kanto basin. At this site, PS-Logging was carried out to the depth of the basement with an S-wave velocity of about 3km/s (Yamamizu, 2004).
We used two event displayed in Figure 4.1. Focal information of the earthquakes used for estimation of S-wave velocity structure at CHBH13 is displayed in Table 4.1. We used transverse component of velocity wave in

inversion. We used band-pass filter at periods from 1 to 5sec. In inversion, populations and generations are 300 and 200, respectively. We assume a 5-layers model. Search limits in inversion for CHBH13 are displayed in Table 4.2. S-wave velocity of the 5th layer is fixed to 2.92km/s.

Comparison between observed and calculated waveforms is displayed in Figure 4.2a and b. The calculated wave agree well with the observed wave from *t1* and *t3*. Comparison of the inverted model and the PS-Logging result is displayed in Figure 4.2c. Although the S-wave velocities in the shallow part are smaller than that of PS-Logging results, the basement depth agrees well with that of the PS-Logging result. The parameter distributions of acceptable models for the inversions at CHBH13 are displayed in Figure 4.3. The threshold was set to be equal to the minimum $E*1.03$ in Figure 4.3a. The threshold was set to be equal to the minimum $E*1.1$ in Figure 4.3b. S-wave velocity and thickness of the 4th layer spreads in a wide area. So the resolution of the 4th layer is lower than those of the other layer.

Comparisons of transfer functions are displayed in Figure 4.4. Observed spectral ratios between surface and bottom of borehole at CHBH13 are calculated by the event focal depth more than 50km. We didn't use above two events (N-1 and N-2). The first and second peaks of the transfer function of SH wave by the inverted S-wave structural model agree well with the observed transfer function. The second peak in the transfer function of the PS logging result is longer than that of the observed transfer function. Using this method, we can estimate the site amplification that is similar to observed one.

5. APPLICATON TO DATA AT STATIONS AROUND LAKE BIWA

We applied our method to actual data at stations around lake BIWA. The basement depths are estimated from 0.2 to 0.3km by Suzuki et al.(2005). Suzuki et al.(2005) estimate the S-wave velocity structure using H/V spectral ratio for surface waves in strong motion records. Focal information of earthquakes used for estimation of S-wave velocity structure are displayed in Table 5.1. Station points and epicenters are displayed in Figure 5.1.We applied this method to the data at SIG002, SIG005 and SIG007. Because the resolution of Q-value is low, b was fixed to 1. Search limits in inversion are displayed in Table 5.2. The S-wave velocity of the 5th layer is fixed to 3.0km/s.

Comparisons between observed and calculated waveforms at SIG002, SIG005 and SIG007 are displayed in Figures 5.2, 5.3 and 5.4, respectively. In these figures, S-wave velocity structures by Suzuki et al.(2005) are also displayed. The depths of the layer having an S-wave velocity more than 1.5km/s at SIG002, SIG005 and SIG007 are about 0.27km, 0.24km and 0.3km, respectively.

Comparisons of the observed H/V spectra and the calculated Rayleigh wave H/V spectra are displayed in Figure 5.5. The observed H/V spectra are calculated by the earthquake records more than Mj6.0. The observed H/V spectra are calculated from coda wave. Although the S-wave velocity structures differ from those by Suzuki et al. (2005) and this study, the peak periods of the H/V spectra of Rayleigh wave are almost equal.

6. CONCLUTIONS

We proposed an inversion method for estimation of a 1D S-wave velocity structure of deep sedimentary layers using S-wave part of earthquake records for evaluating site amplification. We conducted numerical experiments using synthetic data. Although the true S-wave profile is well reconstructed from the inversion, the resolution of Q-value is low.

We applied our method to actual data at Narita in the Kanto basin. Inverted structure is in a good agreement with the S-profile from the PS-logging. The observed transfer function of SH-wave calculated from the spectral ratio between surface and bottom of the borehole agrees with that of the inverted model. The S-wave velocity structures are also retrieved from inversions of earthquake data at stations around Lake Biwa. The basement depths are estimated from 0.2 to 0.3km in the area. The inverted S-wave structures can explain the peak periods of the H/V spectral ratio for surface waves.

REFERENCES

Haskell, N. A. (1960): Crustal reflection of plane SH waves, J. Geophys. Res., 65, 4147-4150.

Hikima, K. and K. Koketsu (2005): Rupture processes of the 2004 Chuetsu (mid-Niigata prefecture) earthquake, Japan: A series of events in a complex fault system, Geophys. Res. Lett., 32, doi:10.1029/2005GL023588.

Horikawa, H., K. Mizuno, T. Ishiyama, K. Satake, H. Sekiguchi, Y. Kase, Y. Sugiyama, H. Yokota, M. Suehiro, T. Yokokura, Y. Iwabuchi, N. Kitada and A. Pitarka1 (2003): A three-dimensional subsurface structure model beneath the Osaka sedimentary basin, southwest Japan, with fault-related structural discontinuities (in Japanese with English abstract), Annual report on active fault and paleoearthquake researches,7, 225-259.

Kudo and Sakaue (1984): Oil-sloshing in the huge tanks at Niigata due to the Nihonkai-Chubu earthquake of 1983(in Japanese with English abstract), Bull. Earthq. Res. Inst. Univ. Tokyo, 59, 361-382

Kurose, T., H. Yamanaka (2006): Joint inversion of receiver function and surface-wave phase velocity of sedimentary layers, Geophysical Exploration (Butsuri-Tansa), 59, 93-101.Mikoshiba and Kinoshita, 1989.

Ludwig, W. J., S. Murauchi, N. Den, P. Buhl, H. Hotta, M. Ewing, M. Asanuma, T. Yoshii and N. Sakajiri (1973): Structure of East China Sea-West Philippine Sea Margin off Southern Kyushu, Japan, J. Geophys. Res., 78, 2526-2536.

Mikoshiba, T and S. Kinoshita (1989): Strong later phases recorded at Fuchu strong-motion array observation during a swarm of 1987 off Fukushima Pref. earthquakes, Report of the National Research Center for Disaster Prevention, 41, 95-104.

Miura, H. and S. Midorikawa (2001): Effects of 3-D Deep Underground Structure on Characteristics of Rather Long-Period Ground Motion – Examination in and around Yokohama City –(in Japanese with English abstract), ,J. Seismol. Soc. Jpn, 54, 381– 395.

Suzuki, H., M. Morino, K. Iwamoto, Y. Liu, H. Fujiwara, and Y. Hayakawa (2005), 3-D subsurface structural model for strong motion simulation around Lake Biwa, southwest Japan (in Japanese with English abstract), J. Seismol. Soc. Jpn, 58, 91– 106.

Yamamizu, F.(2004): Seismic Wave Velocity Structures in Kanto Area as Revealed by the Crustal Activity Observation Well VSP, Technical Note of the National Research Institute for Earth Science and Disaster Prevention, 251, pp75.

Yamanaka, H., K. Seo and T. Samano (1989): Effects of sedimentary layers on surface-wave propagation, Bull. Seism. Soc. Am., 79, 631-64.

Yamanaka, H. and N. Yamada (2006): Modeling 3D S-wave velocity structure of Kanto basin for estimation of earthquake ground motion (in Japanese with English abstract), BUTSURI-TANSA, 59, 549-560.
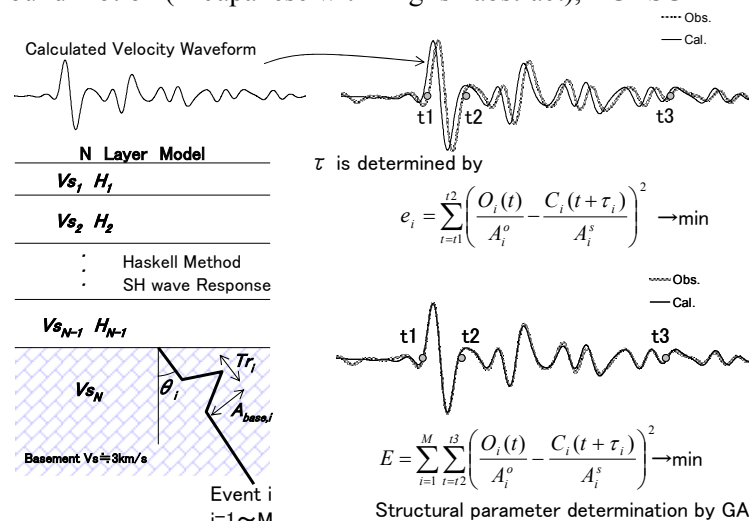
Figure 2.1 Concept of estimation of S-wave velocity structure using a waveform in inversion.

Table 3.1 Search limits in inversion for Model1. Values in parenthesis indicate true model.

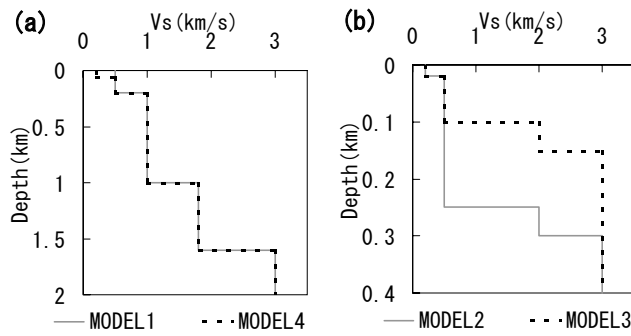| Layer No.	Vs (km/s)	H (km)	Event No.	Tr (s)	Angle (°)	a	b
1lay	0.3–0.7 (0.5)	0.02–0.5 (0.2)	Event1-1	0.9–1.2 (1.0)	0–50 (0)	1–20 (5)	0.3–2.0 (1.0)
2lay	0.6–1.5 (1.0)	0.05–1.0 (0.8)	Event1-2	1.1–1.3 (1.25)	0–50 (30)		
3lay	1.4–2.2 (1.8)	0.1–1.5 (0.6)	Event1-3	1.4–1.6 (1.5)	0–50 (45)		
4lay	3.0 (3.0)	–					

Figure 3.1   S-wave velocity models for numerical experiments. (a) Model 1 and 4 and (b) Model 2 and 3

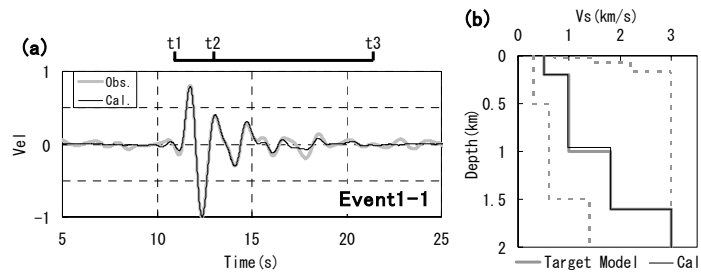
Figure 3.2 Comparisons between observed and calculated waveforms for (a)Evnet1-1. Gray thick lines and black thin lines indicate observed and calculated velocity waveforms, respectively. (b) Comparison between true and inverted models. A gray thick line and black thin line indicate true and inverted velocity structures, respectively. Gray broken lines indicate search areas in the inversion.
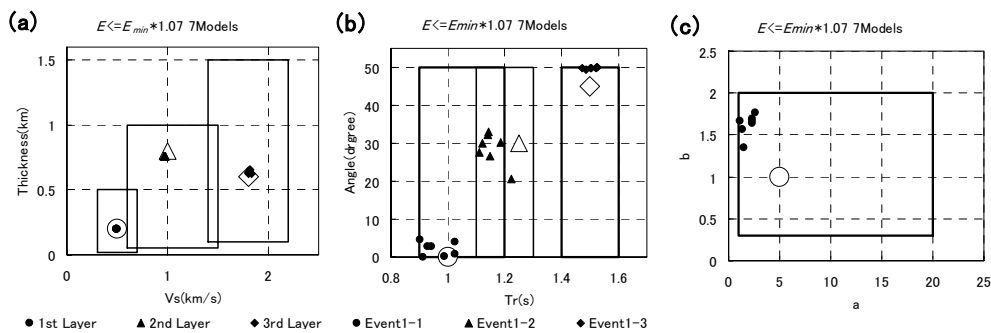

ure 3.3 Parameter distributions of acceptable models for the inversions in numerical experiment for Model1. The threshold was set to be equal to the minimum $E*1.07$. (a) Solid circles, triangles and lozenges indicate S-wave velocity and thickness of the first, second and third layers, respectively. (b) Solid circles, triangles and lozenges indicate Tr and input angle of Event1-1, Event1-2 and Event1-3, respectively. (c) Solid circles indicate a and b for Q-value. Open circles, triangles and lozenges indicate each parameter of true model. Rectangle areas indicate search areas of each parameter.
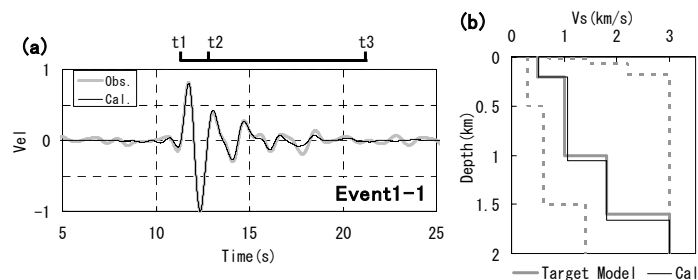

Figure 3.4 The results of the inversion with optimization of $t1$ and $t3$ for Model 1. (a) Comparison between observed and inverted waveforms. (b)Comparison between true and inverted models. Symbols are the same as those of Figure 3.1.
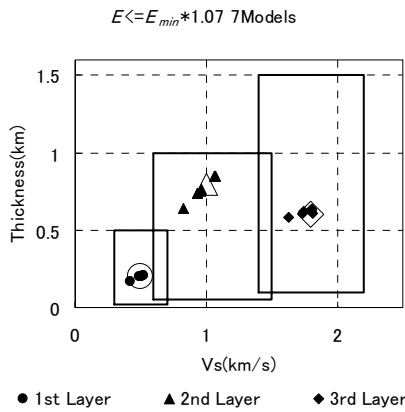
*E<=E$_{min}$*1.07 7Models

Figure 3.5 Parameter distributions of acceptable models for the inversions in numerical experiment with optimization of *t1* and *t3* for Model1. The threshold was set to be equal to the minimum E*1.07. Symbols are the same as those of Figure3.2 (a).
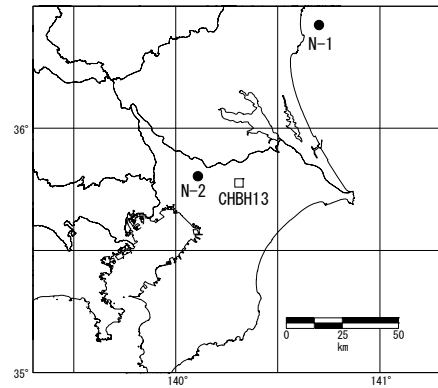

Figure 4.1 Locations of KiK-net station (CHBH13) and epicenters of earthquakes used for estimation of S-wave velocity structure.

Table 4.1 Focal information of earthquakes used for estimation of S-wave velocity structure at CHBH13.

No.	Origine Time		Lon	Lat	Depth(km)	Mj	Epicenter
EvnetN-1	2003/6/9	18:59:38.73	140.7025	36.4230	54.21	4.7	E OFF IBARAKI PREF
EventN-2	2004/4/6	22:05:12.45	140.1083	35.8040	65.18	4.3	NORTHERN CHIBA PREF

Table 4.2 Search limits in inversion for CHBH13

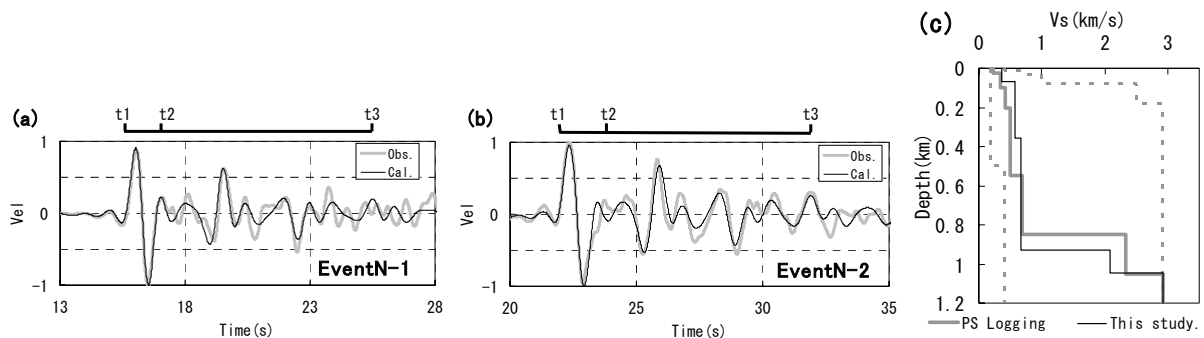| Layer No.	Vs (km/s)	H (km)	Event No.	Tr (s)	Angle(°)	a	b
1lay	0.2-0.4	0.01-0.5	EventN-1	0.8-1.0	0-50	1-20	0.3-2.0
2lay	0.4-0.7	0.02-1.0	EventN-2	1.1-1.3	0-50		
3lay	0.5-1.0	0.05-1.5					
4lay	2.0-2.5	0.1-1.0					
5lay	2.92	–					

Figure 4.2 Comparison between observed and calculated waveforms for (a)EvnetN-1 and (b) EventN-2. A gray thick line and black thin line indicate observed and calculated velocity waveforms, respectively. (c)Comparison of inverted model and PS-Logging result. Solid thin line and gray thick line indicate inverted model and PS-logging result, respectively. Gray broken lines indicate search areas of the inversion.
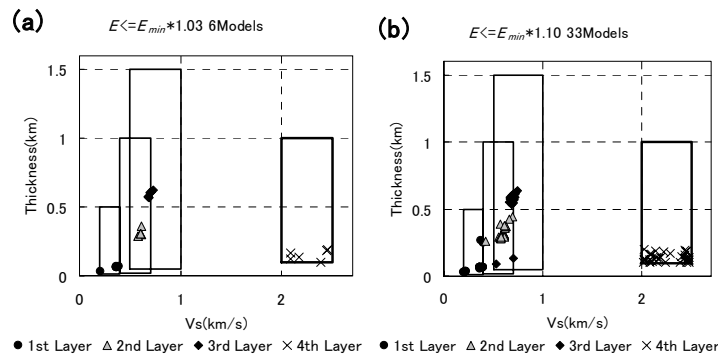
(a) $E <= E_{min}*1.03$ 6Models

(b) $E <= E_{min}*1.10$ 33Models

● 1st Layer △ 2nd Layer ◆ 3rd Layer × 4th Layer   ● 1st Layer △ 2nd Layer ◆ 3rd Layer × 4th Layer

Figure 4.3 Parameter distributions of acceptable models for the inversions at CHBH13. (a) The threshold was set to be equal to the minimum $E*1.03$. (b)The threshold was set to be equal to the minimum $E*1.1$. Circles, triangles, lozenges and crosses indicate the parameter of the first, second, third and forth layers, respectively. Rectangle areas indicate search areas of each parameter.

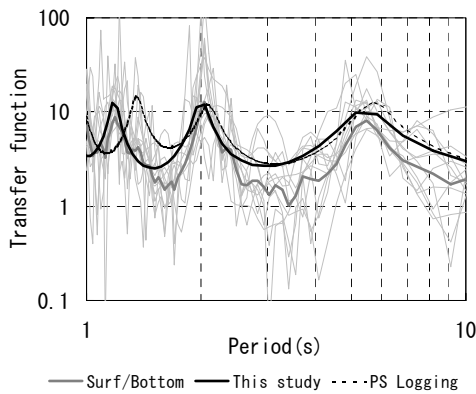— Surf/Bottom —— This study ---- PS Logging

Figure 4.4 Comparison of transfer functions. Thin gray lines indicate observed spectral ratios between surface and bottom of borehole at CHBH13. A gray thick line indicates average of the observed spectral ratios. A black thick line indicates calculated transfer function of SH wave by inverted S-wave structural model in Figure4.2. A black thick line indicates calculated SH wave transfer function by inverted S-wave structural model. A broken line indicates calculated SH wave transfer function of PS logging result.
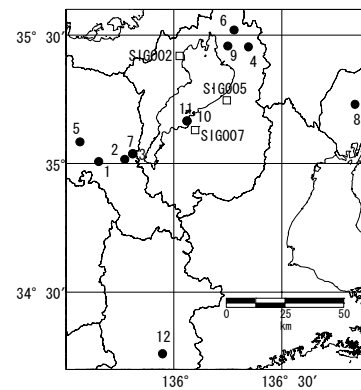
Figure 5.1 Locations of K-NET stations (SIG002, SIG005, SIG007) and epicenters of earthquakes used for estimation of S-wave velocity structures around Lake Biwa.

Table 5.1 Focal information of earthquakes used for estimation of S-wave velocity structure around Lake Biwa. Circles indicate available events at each site.

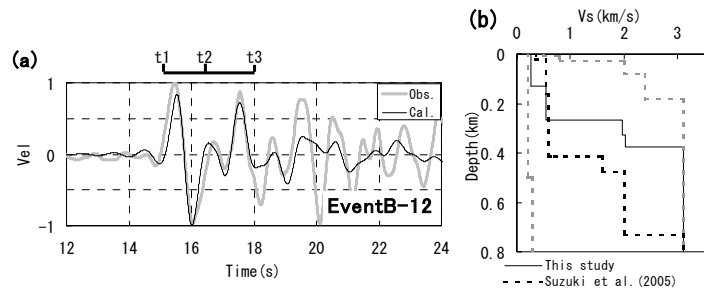| No.	Origine Time	Lon	Lat	Depth (km)	Mj	Epicenter	SIG002	SIG005	SIG007
B-1	1996/05/29 17:37:45.96	135.6513	35.0080	16.55	3.8	KYOTO OSAKA BORDER REG		●	
B-2	1996/07/18 13:44:14.47	135.7723	35.0167	15.19	3.7	KYOTO OSAKA BORDER REG		●	
B-3	2000/05/21 10:42:34.76	135.8087	35.0385	14.41	3.9	KYOTO OSAKA BORDER REG	●		
B-4	2002/09/04 18:06:13.41	136.3458	35.4540	38.52	4.3	SHIGA GIFU BORDER REGION			●
B-5	2003/02/06 02:37:04.48	135.5648	35.0845	15.00	4.2	MID KYOTO PREF		●	
B-6	2004/05/09 04:49:13.11	136.2795	35.5192	10.67	3.4	SHIGA GIFU BORDER REGION	●	●	
B-7	2004/12/01 23:30:23.47	135.8105	35.0392	12.63	4.0	KYOTO OSAKA BORDER REG	●	●	
B-8	2005/12/24 11:01:55.02	136.8402	35.2307	42.96	4.8	CENTRAL AICHI PREF	●		
B-9	2006/01/15 19:54:15.79	136.2502	35.4575	34.9	3.7	SHIGA GIFU BORDER REGION			●
B-10	2007/06/05 06:16:22.24	136.0598	35.1662	11.42	3.2	NW SHIGA PREF		●	●
B-11	2007/07/07 00:35:22.93	136.0622	35.1658	11.31	3.1	NW SHIGA PREF		●	●
B-12	2007/07/16 17:24:19.11	135.9473	34.2613	48.69	4.7	SOUTHERN NARA PREF	●		

(a) EventB-12

(b) Vs (km/s)

Figure 5.2 Comparison between observed and calculated waveforms for (a) EventB-12 at SIG002. A gray thick line and black thin line indicate observed and calculated velocity waveforms, respectively. (b) Black lines and broken line indicate velocity structures with this study and Suzuki et al. (2005), respectively. Gray broken lines indicate search areas in the inversion.
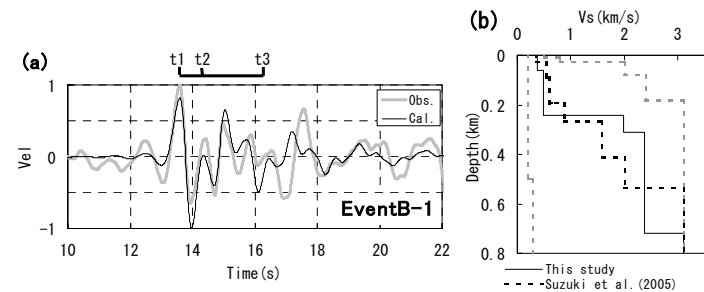
Table 5.2 Search limits in inversion for the sites around Lake Biwa.

Layer No.	Vs (km/s)	H (km)
1	0.2－0.5	0.05－0.6
2	0.3－0.8	0.05－0.6
3	1.5－2.0	0.05－0.5
4	1.8－2.4	0.05－0.5
5	3.1	－

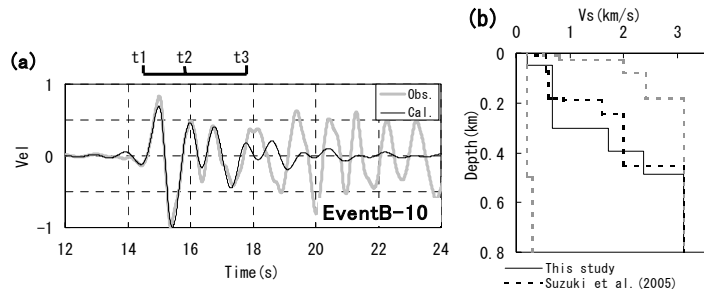Figure 5.3 Same as Figure5.2, but for EventB-1 at SIG005.

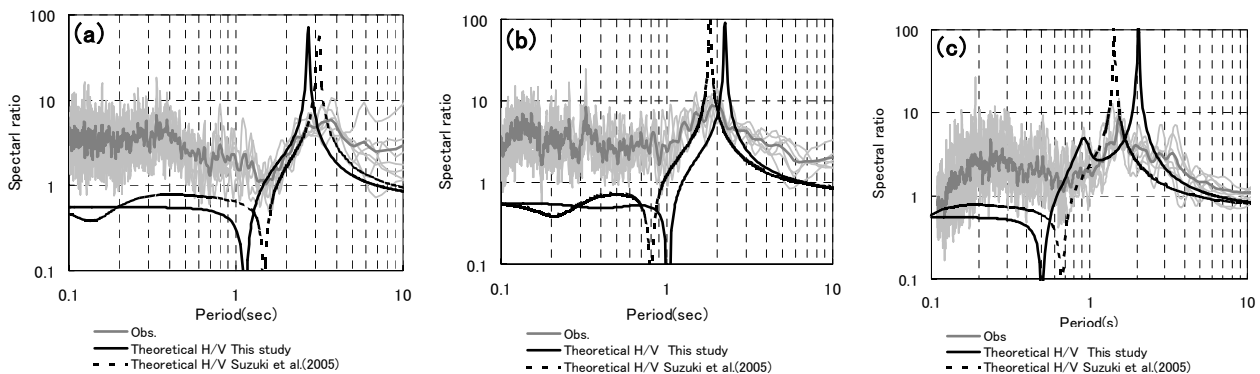Figure 5.4 Same as Figure5.2, but for EventB-10 at SIG007.

Figure 5.5 Comparisons of H/V spectra at (a) SIG002, (b) SIG005 and (c) SIG007, respectively. Gray thin lines and gray thick line indicate observed H/V spectra and averaged H/V spectra, respectively. A black line and black broken line indicate Rayleigh wave ellipticities of fundamental mode by this study and Suzuki et al. (2005).